Theoretical Study of Comb Polymers Adsorption on Solid Surfaces

Anna Sartori,* Albert Johner, Jean-Louis Viovy, and Jean-François Joanny

Department of Molecular Structural Biology, Max Planck Institute for Biochemistry, Am Klopferspitz 18a, 82152 Martinsried (Munich), Germany

Received May 26, 2004; Revised Manuscript Received January 14, 2005

ABSTRACT: We propose a theoretical investigation of the physical adsorption of neutral comb polymers with an adsorbing skeleton and nonadsorbing side chains on a flat surface. Such polymers are particularly interesting as "dynamic coating" matrices for bioseparations, especially for DNA sequencing, capillary electrophoresis, and lab-on-chips. Separation performances are increased by coating the inner surface of the capillaries with neutral polymers. This method allows one to screen the surface charges, thus preventing electro-osmosis flow and adhesion of charged macromolecules (e.g., proteins) on the capillary walls. We identify three adsorption regimes: a "mushroom" regime, in which the coating is formed by strongly adsorbed skeleton loops and the side chains anchored on the skeleton are in a swollen state, a "brush" regime, characterized by a uniform multichains coating with an extended layer of nonadsorbing side chains and a nonadsorbed regime. By using a combination of mean field and scaling approaches, we explicitly derive asymptotic forms for the monomer concentration profiles, for the adsorption free energy and for the thickness of the adsorbed layer as a function of the skeleton and side chains sizes and of the adsorption parameters. Moreover, we obtain the scaling laws for the transitions between the different regimes. These predictions can be checked by performing experiments aimed at investigating polymer adsorption, such as neutron or X-ray reflectometry, ellipsometry, quartz microbalance, or surface force apparatus.

I. Introduction

Polymer adsorption on surfaces is of paramount importance for numerous applications. In material sciences, it is used to control surface properties such as wetting, hardness, or resistance to aggressive environments. It can also have detrimental effects in fouling, alteration of the aspects of materials, and, generally speaking, unwanted changes in surface properties.

Polymer adsorption also gains more and more attention in the field of biology, in which it plays an essential role in biocompatibility, cell adhesion, containers and instruments contamination, and bioanalytical methods. Many proteins, in particular, have a strong amphiphilic character, and these tend to adsorb easily to surfaces bearing charges or hydrophobic domains. Strong efforts have been continuously made, in the last 20 years, to develop surface treatments able to prevent unwanted adsorption of biomolecules in a water environment. The proposed solutions often amount to treating the surface with specially chosen proteins, oligomers, or polymers. In most cases, a very hydrophilic polymer is required. Numerous polymers have been proposed in this context, including polysaccharides, poly(vinyl alcohol), and the very popular poly(ethylene oxide).

Depending on the application, two different approaches can be envisaged: either polymer grafting onto the surface by one or several covalent bonds (see, e.g., ref 1, etc.) or spontaneous adsorption. The latter solution is in general easier to implement, and the regeneration of a fouled or damaged surface is easier. However, the adsorbed polymer layer is in general more fragile than a covalently bonded surface, and the adsorption approach puts constraints on the chemical nature and architecture of the polymers, which can be difficult to fulfill. In particular, surface coatings in the field of biology must in most cases be hydrophilic. Since very hydrophilic polymers most often do not adsorb spontaneously onto surfaces in a water environment (their free energy in the solvated state is very low), some "tricks" must be developed.

One efficient way to favor adsorption of a hydrophilic layer is to use block copolymers, with one (or several) hydrophilic block, and one or several blocks playing the role of an anchor. In particular, diblock and triblock copolymers or oligomers, such as alkyl−poly(ethylene oxide) diblocks, or poly(ethylene oxide)−poly(propylene oxide)−poly(ethylene oxide) triblocks, were used with success for several applications. They are far to be a universal solution to unwanted adsorption and wall-interactions of biomolecules. In particular, they seem rather unsuccessful in the field of capillary electrophoretic separations.

This bioanalytical method has been widely popularized by the large genome projects (the human genome project, and most of the current genome projects rely mainly on capillary array electrophoresis for DNA sequencing[2]) and its importance is bound to increase further with the development of massive "post-genome" screening and "lab-on-chips" methods for research and diagnosis.[3,4] In capillary electrophoresis, analytes are separated by electrophoretic migration under a high voltage (typically 200−300 V/cm) in a thin capillary (typically 50 μm i.d.). Interactions of the analytes with the walls are of paramount importance, because the interactions can lead to considerable peak trailing and because the interactions can cause electro-osmosis, a motion of the fluid induced by the action of the electric field on the excess of mobile free charges in the vicinity of a charge surface (see, e.g., ref 5).

Consider an infinitely long pipe filled with an electrolyte, with a nonvanishing ζ potential (the most common situation when a solid is in contact with an electrolyte). The surface has a net charge, and a Debye layer of counterions forms in the fluid in the vicinity of

* E-mail: sartori@biochem.mpg.de. Fax: +49 (89) 85782641.

10.1021/ma0489624 CCC: $30.25
Published on Web 03/17/2005

this surface in order to minimize the electrostatic energy. In buffers typically used in electrophoresis, the Debye layer has a thickness of a few nanometers. Choosing for definiteness a negatively charged surface, such as e.g. glass in the presence of water at pH 7, the Debye layer is positively charged. Applying an electric field along the pipe, the portion of fluid contained in the Debye layer is dragged toward the cathode. Solving the Stokes equation with the boundary condition of zero velocity at the surface leads to a "quasi-plug" flow profile, with shear localized within the Debye layer and a uniform velocity in the remainder of the pipe. If the electrical charge on the surface is nonuniform, due for example to a local adsorption of biopolymers, the velocity at the wall, which is imposed by the local zeta potential, is also nonuniform. In such case, the flow is no more a plug flow, and there are hydrodynamic recirculations detrimental to the resolution.[6] Electroosmosis generally has very dramatic consequences on the performance of practical electrophoretic separations, and it must be thoroughly controlled. Polymers at the interface can play a double role in circumventing electroosmosis: by preventing unwanted adsorption of analytes or impurities contained in the electrophoretic buffer and by decoupling the motion at the wall from the motion of the bulk fluid. For this, the polymer layer must be thicker than the Debye length. Different strategies, using either covalently bonded polymers (see e.g., ref 7) or reversibly adsorbed polymers (so-called "dynamic coating"; see, e.g., refs 8 and 9), have been developed. The use of relatively short copolymers[10,11] has been rather deceptive, probably because they lead to rather thin layers and because the adsorption free energy of an individual chain is too low to resist the rather aggressive conditions encountered during electrophoresis in strong fields (in particular high shear at the wall). These oligomers need to be present in the solution at a high concentration, to yield sufficient dynamic coating. Presently, the most efficient applications of dynamic coating have involved poly(dimethyl acrylamide) (PDMA)[12] or copolymers of this polymer with other acrylic monomers.[13] This polymer seems to present an interesting affinity to silica walls, thanks to the presence of hydrogen bonding, while remaining soluble enough in water to behave as a sieving matrix. It was demonstrated,[14] however, that its reduced hydrophilicity as compared with, e.g., acrylamide,[15] results in poorer separation performance, probably due to increased interactions with the analytes.

Recently, we proposed[16] a new family of block copolymers comprising a very hydrophilic poly(acrylamide) (PA) skeleton and PDMA side chains, as dynamic coating sieving matrices for DNA electrophoresis. These matrices provide an electro-osmosis control comparable to that of pure PDMA, while allowing for better sieving. A large range of different microstructures can be conceived and constructed, by varying the length and chemical nature of the grafts and of the skeleton and the number of grafts per chain. The aim of the present article is to investigate theoretically the adsorption mechanisms and the structure of adsorbed layers of polymers with this type of microstructure, to better understand the properties, and to provide a rational basis for further experimental investigations and applications. The adsorption of homopolymers, of di- or triblock copolymers, and random copolymers of adsorbing and nonadsorbing polymers has been investigated theoretically.[17−25] To our knowledge, however, the case of a comb polymer with different adsorption properties on the skeleton and on the grafts has never been considered. We address this problem here, generalizing on previous work on random and triblock copolymers.

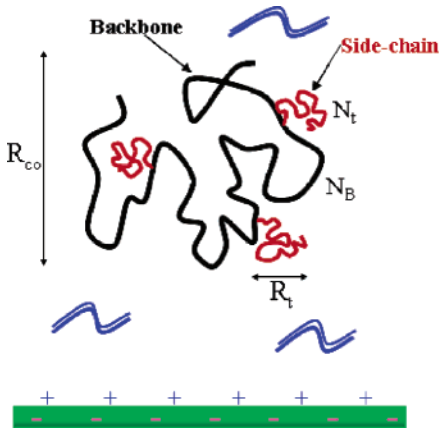

Figure 1. Comb-copolymer in solution, made of an adsorbing backbone made of p blocks of N_B monomers each and with p nonadsorbing side chains of N_t monomers each. The total number of monomers is $N = p(N_B + N_t)$ (with $p = 3$), and the gyration radius is $R_{co} \sim aN^{1/2}$, a being the monomer size.

The architecture of the paper is as follows: In section II, we investigate the adsorption of comb polymers with adsorbing backbone and nonadsorbing side chains. In section II.A, we present a mean field model for the analysis of the adsorption of combs in the limit of small side chains, i.e., in the mushroom regime ($N_t \ll N_B$, where N_t and N_B are the number of monomers of a nonadsorbing side chain and of the corresponding adsorbing backbone chain section, respectively).

In section III, we use a scaling approach to describe the adsorption of comb polymers both in the mushroom and in the brush regime (i.e. in the limit of large side chains) and the crossover between these two regimes.

II. Adsorption of Comb Polymers with Adsorbing Backbone and Nonadsorbing Side Chains: Mean Field Theory

In this section, we give a mean field description of the adsorption of comb polymers with adsorbing backbone and nonadsorbing side chains onto a flat solid substrate. The combs have an adsorbing backbone B, made of p blocks of N_B monomers each with gyration radius $R_B \sim aN_B^{1/2}$, on which are grafted p nonadsorbing T side chains, of N_t monomers each and of gyration radius $R_t \sim aN_t^{1/2}$, where a is the monomer size. We study the adsorption behavior of combs, which is monitored by the mass ratio between the adsorbed backbone B and the nonadsorbing side chains T.

We treat at the mean field level the case of small side chains and low grafting density. This leads to a "mushroom" configuration for the adsorbed comb polymers, having the backbone adsorbed on the surface and the side chains dangling from the backbone, with weak steric interaction between them (see Figure 1). Our analysis is based on the idea of describing the combs as linear chains having "triblock copolymers" as renormalized monomers (see Figure 2). By exploiting the known solution for linear chains adsorbing from a dilute solution on a flat surface, one can directly derive the comb polymers adsorption profile, by integrating out the triblock copolymers degrees of freedom.

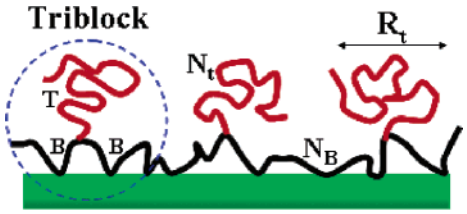

Figure 2. Mushroom configuration for a comb polymer, made out of p ($p = 3$) triblock subunits. Each triblock is made of two backbone blocks of $N_B/2$ monomers and of one anchored side chain of N_t monomers and gyration radius R_t (indicated in the figure with the letters B and T, respectively).

A. Mean Field Theory of Triblock Copolymer Adsorption. Consider a dilute solution of triblock copolymers ($p = 1$), with an adsorbing backbone made of two large adsorbing blocks of $N_B/2$ monomers each, and one nonadsorbing small side chain, of N_t monomers, with $N_B \gg N_t$. The total number of monomers is $N = N_B + N_t \sim N_B$. We solve the problem in the ground state dominance approximation, applicable to the case where the polymers have large enough molecular weights and there is only one bound state of energy $E_o < 0$. A detailed description of the triblock copolymer adsorption behavior and configurations can be obtained by deriving the polymer partition function $Z_N(z)$, in the case where one backbone end-point is fixed at position z above the adsorbing surface ($z = 0$) and the other end-point is free. The partition function $Z_n(z)$ is a solution of the so-called Edwards equation[17,19]

$$\begin{cases} -\dfrac{\partial Z_n(z)}{\partial n} & = -\dfrac{\partial^2 Z_n(z)}{\partial z^2} + U(z)Z_n(z) \\ -\dfrac{\partial(\ln Z_n(z))}{\partial z}\Big|_{z=0} & = -\dfrac{1}{b} \end{cases} \tag{1}$$

where the unit length has been defined as $a/\sqrt{6}$ and a is the monomer size. The boundary condition imposed at the surface is a good approximation of the surface potential effect, if we neglect the details of the concentration profile close to the surface. The extrapolation length b gives a measure of the strength of the adsorption. We build here the partition function of the adsorbed combs starting from the known solution $Z^o_N(z)$ for the adsorption of a linear chain of N monomers, which is also a solution of eq 1. Far from the surface the chain is free and can assume all configurations in space, $Z^o_N(z \gg R_B) = 1$. We choose the normalization of the partition function to be one when the chain reduces to one monomer, $Z^o_0(z) = 1$.

The mean field effective potential experienced by the adsorbed chains can be expressed self-consistently as

$$U(z) = \Phi(z) - \Phi_b = v\,(c(z) - c_b) \tag{2}$$

where $\Phi(z)$ is the monomer volume fraction, equal to the bulk value Φ_b sufficiently far from the surface, v is the excluded volume parameter ($v \sim a^3 > 0$ in a good solvent) and $c(z)$ is the monomer concentration.

The partition function Z^o_N can be split into two contributions: the adsorbed states contribution $Z^{o^a}_N$, arising from chains having at least one monomer adsorbed onto the surface, and a free chain contribution $Z^{o^f}_N$, arising from chains with no adsorbed monomers, so that $Z^o_N = Z^{o^a}_N + Z^{o^f}_N$. We can derive an expression for both components as independent solutions of the Edwards equation, with appropriate boundary conditions (see section II.A). Starting from the knowledge of $Z^{o^a}_N$ and of $Z^{o^f}_N$ (which from now on we denote as Z^o_N and Z^f_N) for the adsorption of a linear chain of N monomers, we build the partition function of a triblock copolymer, by neglecting the effect of free triblock copolymer chains on the adsorption profile near the surface. The nonadsorbing side chains contribute as a small perturbation to the adsorption profile.

B. Backbone Partition Function. For the adsorption of a linear backbone, made of N_B monomers, the ground state dominance approximation amounts to considering the limit of very large molecular weights, $\epsilon_o N_B \gg 1$, where ϵ_o is the absolute value of the contact free energy per monomer ($\epsilon_o = |E_0| = -E_0$). This implies that the expansion of $Z^o_{N_B}(z)$ in terms of the normalized eigenvectors $\psi_i(z)$ ($\int_0^\infty dz\ \psi_i\psi_j = \delta_{ij}$) and of the eigenvalues of eq 1 is dominated by the first ground-state term

$$Z^o_{N_B}(z) \sim \sum_i k_i\,\psi_i(z)e^{\epsilon_i N_B} \sim k_o\psi_o(z)e^{\epsilon_o N_B} + \ldots\ \epsilon_o N_B \gg 1 \tag{3}$$

where ψ_o is a solution of

$$0 = -\frac{\partial^2\psi_o(z)}{\partial z^2} + (U(z) + \epsilon_o)\,\psi_o(z) \tag{4}$$

with boundary condition

$$\frac{-1}{b} = \frac{1}{\psi_o}\frac{\partial\psi_o}{\partial z}\Big|_{z=0} \quad \text{and} \quad \psi_o(z \to \infty) = 0 \tag{5}$$

The amplitude k_o is fixed by imposing the backbone end-points conservation relation (see also ref 26)

$$\frac{\Gamma_o}{N_B} = \int_0^\infty \frac{\rho_e(z)}{2}\,dz \tag{6}$$

where the parameter Γ_o represents the surface coverage (number of monomers per unit surface) and $\rho_e(z)$ is the end-points monomer density. Close to the surface, the end-points density $\rho_e(z)$ is proportional to the total partition function of the linear backbone, $\rho_e(z) \simeq 2\,\Phi_b Z^o_{N_B}(z)/N_B$. The adsorbance Γ_o is directly obtained by integrating the monomer volume fraction $\Phi(z)$, which can be expressed as the sum of the loops and of the dangling tails contribution, $\Phi(z) = \Phi_l(z) + \Phi_t(z)$, with

$$\Phi_l(z) = \frac{\Phi_b}{N_B}\int Z^o_{N_B-n}(z)Z^o_N(z)\,dn \tag{7}$$

giving $k_o = \int \psi_o$, $\Phi_l \sim \Gamma_o\psi_o^2$, and $\Gamma_o = \Phi_B k_o^2 e^{\epsilon_o N_B}$.

By taking into account the contributions of the free dangling backbone ends, one can define the order parameter $\varphi(z) \sim \int Z^f_{n_B}(z)e^{-\epsilon_o N_B}\,dn_B$, which is the solution of the following equation:

$$1 = -\frac{\partial^2\varphi(z)}{\partial z^2} + (U(z) + \epsilon_o)\,\varphi(z) \tag{8}$$

derived from eq 1 for $Z^f_{N_B}(z)$, with boundary condition $\varphi(0) = 0$. One can solve the differential equations for

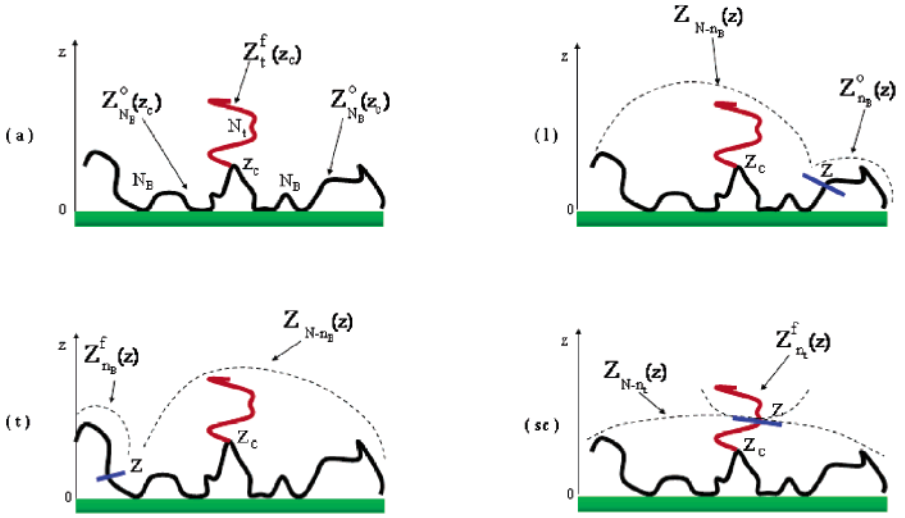

Figure 3. Representation of the construction of the triblock total partition function Z (a) and of the (l) backbone's loops (l) tails (t) and side chains (sc) contributions to the triblock copolymer monomer volume fraction Φ^{TB}, starting from the knowledge of the partition functions for the adsorbed backbone blocks, Z^o and for the dangling tails, Z_t^f (z_c is the triblock's core position above the adsorbing surface).

$\psi_o(z)$ and $\varphi(z)$ and express the effective potential U (or equivalently the monomers volume fraction Φ in the case of dilute solutions) as

$$\Phi = \Phi_l + \Phi_t = \Gamma_o {\psi_o}^2 + B_o(\sqrt{\Gamma_o}\psi_o)\varphi \tag{9}$$

where

$$\sqrt{\Gamma_o}\,\psi_o = \begin{cases} \sqrt{2}(z+b)^{-1} & 0 < z < z^* \\ \sqrt{2}(N_B b)\, z^{-4} & z^* < z < \lambda_o \end{cases} \tag{10}$$

$$\varphi = \begin{cases} z^2/3\, \log(z/z^*) & 0 < z < z^* \\ z^2/18 & z^* < z < \lambda_o \end{cases}$$

with $z^* \sim (N_B b\, \ln(N_B/b^2))^{1/3}$, $\Gamma_o \sim 2/b$, $k_o = \sqrt{2/\Gamma_o}\, \log(z^*/b) \sim 1/3\, \sqrt{b}\, \log(N_B/b^2)$ and $B_o = 2\, \sqrt{\Gamma_o}/(N_B k_o)$. The value ϵ_o of the ground-state energy can be expressed as

$$\epsilon_o = \frac{1}{N_B} \ln\left[\frac{\Gamma_o}{\Phi_B\, {k_o}^2}\right] \sim \frac{1}{N_B} \ln\left[\frac{2}{\Phi_B\, b^2}\right] \tag{11}$$

The parameter $\lambda_o \sim e_o^{-1/2}$ is the average thickness of the adsorbed layer.

The nonadsorbing side-chain states are described by the "free states" function $Z^f_{N_t}(z) = Z^f_t(z)$ (with $Z^f_t(z=0) = 0$ and $Z^f_t(z \to \infty) = 1$) of a linear nonadsorbed chain of N_t monomers, with the constraint of having one end-point anchored at the middle of the adsorbing backbone at $z = z_c$, the other end point being integrated out (see Figure 3). The nonadsorbing side chains feel a strong entropic repulsion at the surface within a layer of thickness $R_t \sim aN_t^{1/2}$, where R_t is their radius of gyration. Thus, for $0 \le z \le R_t$, the probability of finding "free" side chains is very low, $Z^f_t(z) \ll 1$, while for $z > R_t$ one has $Z^f_t(z) \sim 1$. A detailed calculation of the propagator and of the partition function of free chains is given in Appendix C, assuming that the side chains only give a small contribution to the total concentration profile; for simplicity, we only give here scaling arguments.

Close to the surface, the most important contribution to the adsorption profile comes from the central monomers of the side chains,[19] meaning that $Z^f_t(z) \sim \psi^f(z)$,

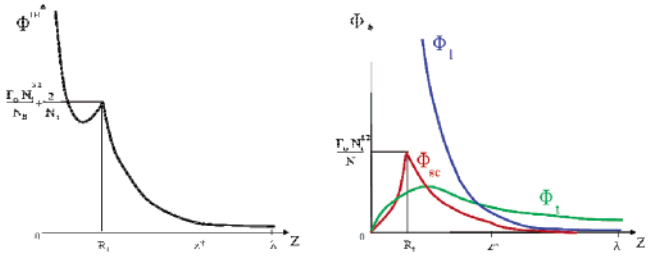

Figure 4. Triblock's monomer volume fraction $\Phi^{TB}_{sc} = \Phi_l + \Phi_t + \Phi_{sc}$: loops ($\Phi_l(z)$), tails ($\Phi_t(z)$), and side chains ($\Phi_{sc}(z)$) contributions.

where $\psi^f(z)$ describes "free" (nonadsorbing) states and satisfies the same equation as $\psi_o(z)$, but with different boundary conditions at the surface, $\psi^f(0) = 0$. For $0 \le z \le R_t$, one can express $\psi^f(z)$ as a function of $\psi_o(z) \sim 1/z$, $\psi^f(z) = \psi_o \int_d^z {\psi_o}^{-2}\, dz \sim z^2$, so that

$$\psi^f(z) \sim \begin{cases} \dfrac{z^2}{{R_t}^2} & z \le R_t \\ 1 & R_t < z \le \lambda_o \end{cases} \tag{12}$$

C. Triblock Copolymer Partition Function. We now derive the triblock copolymer partition function $Z_N(z) \sim k'\psi_o(z) e^{\epsilon N_B}$ (where k' is a constant to be determined and ϵ is the adsorption energy per monomer of the triblock, with $\epsilon > \epsilon_o$) by proceeding analogously to the case of a linear chain and taking into account the constraint of having a nonadsorbing side chain anchored at the midpoint of the adsorbing backbone. We start by deriving the total partition function for a triblock copolymer, which is built from the knowledge of the linear backbone partition function $Z^o_{N_B/2}$ and the partition function of the anchored side chains Z^f_t:

$$Z = \int_0^{+\infty} dz_c \int_0^{+\infty} dz\, Z^o_{N_B/2}(z, z_c)\, Z^f_t(z_c)\, Z^o_{N_B/2}(z_c) = Z^o\, \frac{e^{(\epsilon-\epsilon_o)N_B}}{\Gamma_o R_t} \tag{13}$$

where z_c is the vertical coordinate of the core (i.e. the side-chain anchoring point) above the surface (see Figure 2), $Z^o_{N_B/2}(z, z_c) = \psi_o(z)\ \psi_o(z_c)e^{\epsilon N_B/2}$ is the partition function of an adsorbing backbone block with one end at z_c and one end at z, $Z^f_t(z_c)$ is the partition function of the nonadsorbing side chains with one end at $z = z_c$, and $Z^o = {k_o}^2 e^{\epsilon_o N_B}$. By combining the classical chemical potential balance for a triblock and a linear chain ($\Phi_b/N = \Gamma/(NZ)$), one obtains

$$\ln\left(\frac{\Gamma}{\Gamma_o}\right) - N_B(\epsilon - \epsilon_o) + \ln(\Gamma_o R_t) = 0 \qquad (14)$$

Assuming again that the side chains give only a small perturbation to the total concentration in the adsorbed layer, one can approximate the triblock copolymer surface coverage Γ by the linear chain surface coverage, $\Gamma \sim \Gamma_o$, leading to the following expression for the triblock copolymer ground-state energy:

$$\epsilon = \epsilon_o + \frac{1}{N_B}\ln(\Gamma_o R_t) \qquad (15)$$

The density of junction points of a triblock copolymer at position z_c above the adsorbing surface can be built using similar arguments to those used for the total partition function. Starting from the single chain partition functions Z^f_t and $Z^o_{N_B/2}$, $\rho_c^{TB}(z_c) = \Phi_b Z^f_t(z_c) Z^o_{N_B/2}{}^2(z_c)/N$, one gets

$$\rho_c^{TB}(z_c) = \begin{cases} \dfrac{\Gamma_o}{N_B R_t} & z_c < R_t \\ \dfrac{\Gamma_o R_t}{N_B} z_c{}^{-2} & R_t < z_c < z^* \\ \Gamma_o N_B R_t z_c{}^{-8} & z^* < z_c < \lambda \end{cases} \qquad (16)$$

with $\int \rho_c^{TB}(z)\ dz = \Gamma_o/N_B$.

The junctions of the adsorbed triblock copolymers are therefore confined close to the surface; as they must belong to the loops of the backbone chains, their density in the region where the concentration is dominated by monomers belonging to tails is extremely low. Our analysis holds as long as the gyration radius of the side chains R_t (which gives a measure of the thickness of a depletion layer close to the surface) remains smaller than z^*, i.e. for

$$N_t \le N_B{}^{2/3} \qquad (17)$$

For $N_t \ge N_B{}^{2/3}$ the surface coverage is dominated by the side chains contribution and the side chains gyration radius becomes comparable to the thickness of the loops adsorbed layer, $R_t \sim z^*$. This means that the side chains contribution to the monomer volume fraction can no longer be treated as a perturbation. We can infer that this condition identifies the crossover from "mushroom" ($N_t < N_B{}^{2/3}$) to "brush" ($N_t > N_B{}^{2/3}$) configuration for the adsorbed triblock copolymers. A more rigorous derivation of this statement is obtained at the end of section II.D.1.

D. Monomer Volume Fraction. To get the monomer concentration profiles, we need to evaluate the effective potential felt by the adsorbed chains. For sufficiently diluted solutions, Φ_b can be neglected and thus $U(z) \sim \Phi(z)$. The triblock copolymer partition function $Z_N(z)$ can be expressed by splitting the chain into two parts and by summing over all possible distinct configurations (see Figure 3):

$$\Phi(z) = \frac{\Phi_b}{N_B}\sum \int dn\ Z_{N-n}Z_n \sim \Phi_l(z) + \Phi_t(z) + \Phi_{sc}(z) \qquad (18)$$

where "l", "t" and "sc" stand for loops, tails, and side chains contribution, respectively and

$$\Phi_l(z) = \frac{\Phi_b}{N_B}\int_o^{N_B} dn_B \int_o^{+\infty} dz_c\ Z^o(z_c) Z^f_t(z_c) Z^o(z, z_c)\ Z^o(z) = \Gamma_o {\psi_o}^2(z)$$

$$\Phi_t(z) = \frac{2\ \Phi_b}{N_B}\int_o^{N_B} dn_B \int_o^{+\infty} dz_c\ Z^o(z_c) Z^f_t(z_c) Z^o(z, z_c) Z^f_{n_B}(z) = \frac{2\Gamma_o}{N_B k_o}\psi_o(z)\ \varphi(z)$$

$$\Phi_{sc}(z) = \frac{\Phi_b}{N_B}\int_o^{N_t} dn_t \int_0^{\infty} dz_c\ Z^o(z_c) Z^o(z_c) Z^f_t(z, n_t|z_c)\ Z^f_t(z, N_t - n_t) \qquad (19)$$

where $Z^f_t(z_w, n|z_a)$ is the partition function of an nonadsorbed strand of n monomers starting at z_a and ending at z_w, $Z^f_t(z_w, n)$ is obtained after integration of $Z^f_t(z_w, n|z_a)$ over z_a. These partition functions are discussed in Appendix C. The expressions (eq 19) for the loops and tails contributions to the total monomer volume fraction for a triblock copolymer of $N \sim N_B$ monomers are the same as the one found for the adsorption of a linear polymer chain of N_B monomers. For the side chains monomer volume fraction $\Phi_{sc}^{TB}(z)$, one finds (see Figure 5):

$$\Phi_{sc}^{TB}(z) = \begin{cases} \dfrac{\Gamma_o}{N_B R_t} & z^2 \quad d < z < R_t \\ \dfrac{\Gamma_o {R_t}^3}{N_B} & z^{-2} \quad R_t < z < z^* \\ \Gamma_o {R_t}^3 N_B & z^{-8} \quad z^* < z < \lambda \end{cases} \qquad (20)$$

where λ is the average thickness of the triblock copolymer adsorbed layer. Close to the wall, $d < z < R_t$, where the side chains are depleted, the side-chain volume fraction is constructed from chemically close junction points, each of which contributes z^2 monomers (one blob). Further from the wall, the side-chain density follows the junction point density (with the normalization factor N_t). At short distances, in the adsorbed loops layer, $\Phi_l(z)$ dominates over the other contributions, at large distances, $\Phi(z) \sim \Phi_t(z)$. As for linear chain adsorption, the characteristic length z^* represents the length-scale inside the adsorbed layer (where the adsorption energy ϵ is negligible compared to the effective potential $U(z)$), at the crossover from the loops-dominated layer to the tails dominated layer:

$$z^* \sim \left[Nb\ \ln\left(\frac{N_B}{b^2}\right)\right]^{1/3} \sim (N_B b)^{1/3} \qquad (21)$$

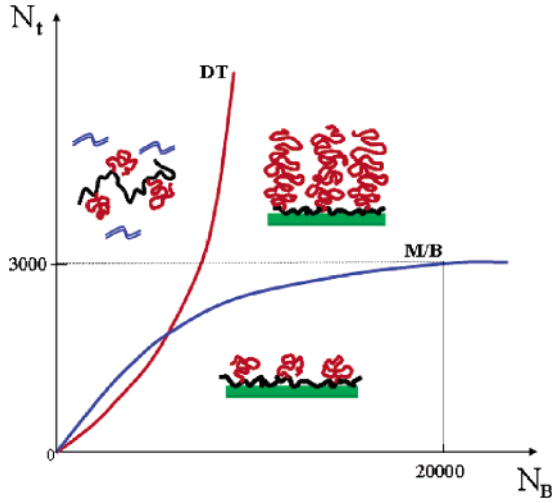

Figure 5. Phase diagram for a comb polymer with an adsorbing backbone made of p blocks of N_B monomers each and nonadsorbing side chains of N_t monomers each. The dashed curve represents the mushroom to brush configuration threshold (M/B) while the solid curve represents the desorption threshold (DT).

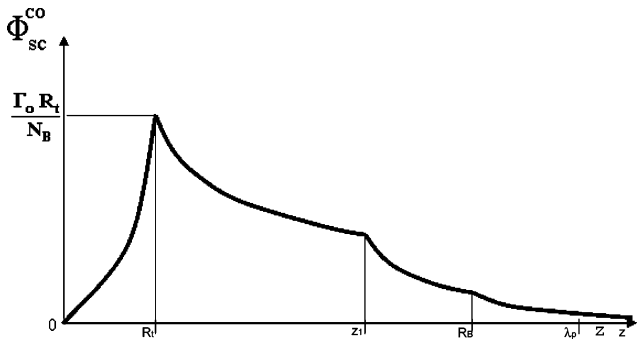

Figure 6. Combs side chains monomer volume fraction, $\Phi_{sc}^{co}(z)$.

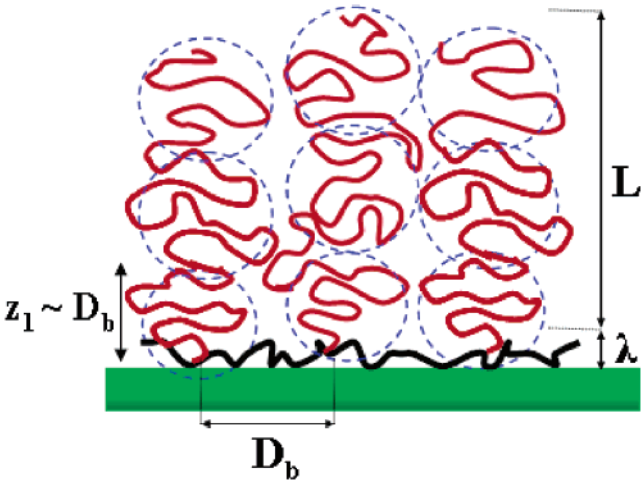

Figure 7. Brush regime for a comb polymer with an adsorbing backbone made of p blocks of N_B monomers each and with p nonadsorbing side chains of N_t monomers each, with $N_t \gg N_B$.

which is the same as the one found for the adsorption of a linear chain of N_B monomers.

The thickness of the adsorbed triblock copolymer layer $\lambda \sim e^{-1/2}$ is smaller than the thickness of a linear polymer adsorbed layer:

$$\lambda = \lambda_o\left[1 + \lambda_o{}^2 \frac{\ln(\Gamma_o R_t)}{N_B}\right]^{-1/2} \tag{22}$$

where

$$\lambda_o = \left(\frac{N_B a^2}{6}\right)^{1/2} \ln\left(\frac{1}{\Phi_b b^2}\right)^{-1/2} \tag{23}$$

If N_t increases, λ decreases, as the adsorption is partially prevented by the presence of the side chains.

From the complete expression for the triblock copolymer volume fraction $\Phi(z)$ (see eqs 18−20), one can calculate the correction to the surface coverage (of backbone monomers) due to the side chains:

$$\Gamma = \Gamma_o\left[1 - \frac{2}{\Gamma_o\lambda} + \frac{N_t}{N_B}\left(2 - \frac{R_t}{z^*}\right)\right] \tag{24}$$

1. From Triblock Copolymers to Combs. Once the adsorption profiles in triblock copolymer adsorbed layers are known, it is straightforward to extend the study to comblike architectures. The combs are linear polymers made of p subunits ($p \geq 1$), which are triblock copolymers with an adsorbing backbone of N_B monomers and size $R_B = N^{1/2}a$ and one nonadsorbing side chain of N_t monomers, with $N_t \ll N_B$. The total number of monomers per comb is $N = p(N_B + N_t) \sim pN_B$.

Far from the adsorbing surface, i.e. for $z \gg R_B$, the comb polymer can be seen as a chain of blobs, each being a triblock copolymer. The density of cores (branching points) and the volume fraction of side chain monomers are therefore $\rho_c(z) = 2z^{-2}/N_B$ and $\Phi_{sc}(z) = 2N_t z^{-2}/N_B$. Close to the surface, eq 20 for triblock copolymer adsorption correctly predicts the structure of the comb side chains adsorption profile $\Phi_{sc}(z) = (\Gamma_o R_t{}^3/N_B)z^{-2}$. These two predictions cannot crossover smoothly. There is therefore an intermediate regime involving a new length scale. There is actually a strong constraint that loops smaller than N_B monomers cannot contain more than one branching point. The profile given by eq 20 is thus valid only up to a distance z_1 where each loop comprises a number of side chains of order one. One can estimate the fraction x of loops of size z that contain one side chain, $x = \rho_c/\rho_l$, where the loops density ρ_l is given by the monomer density divided by the number of monomers per loop $g(z) \sim z^2$ (Gaussian loops), $\rho_l(z) \sim z^{-4}$. This fraction is smaller than one if $z < z_1$, where

$$z_1 = \left(\frac{N_B}{N_t{}^{1/2}}\right)^{1/2} \tag{25}$$

At distances $z_1 < z < R_B$, all loops contain a branching point and $x \sim 1$; i.e., $\rho_c(z) \sim \rho_l(z)$. This description holds as long as the adsorbed combs are in a mushroom regime, i.e., for $R_t < z_1 < R_B$, which leads to the same threshold derived at the end of section II.C for the crossover from a mushroom to a brush configuration for the adsorbed triblock copolymers:

$$N_t < N_B{}^{2/3} \tag{26}$$

Table 1. Mean Field Branching Point Density $\rho_c(z)$ and Monomer Volume Fraction $\Phi_{sc}(z)$ for an Adsorbed Comb Polymer (Where z Is the Vertical Coordinate above the Adsorbing Surface)

	$0 \le z \le R_t$	$R_t \le z \le z_1$	$z_1 \le z \le R_B$	$R_B \le z \le \lambda_p$
$\rho_c(z)$	$\Gamma_o/(N_B R_t)$	$(\Gamma_o R_t/N_B)z^{-2}$	$\Gamma_o z^{-4}$	$(\Gamma_o/N_B)z^{-2}$
$\Phi_{sc}^{co}(z)$	$(\Gamma_o/(N_B R_t))z^2$	$(\Gamma_o R_t^3/N_B)z^{-2}$	$\Gamma_o N_t z^{-4}$	$(\Gamma_o N_t/N_B)z^{-2}$

The structure of the adsorbed layer is mainly determined by the small loop structure close to the wall which is the same for comb and triblock copolymers. In particular, one has that the monomer chemical potential in the case of combs ϵ_p is related to the one for triblock monomers ϵ by $p\epsilon_p \sim \epsilon$. This gives the adsorbed layer thickness of a comb polymers comprising p blocks, $\lambda_p = \sqrt{p}\lambda$ where λ is given by eq 22. In Table 1 we present a summary of the mean field behavior of the comb polymers branching point density and monomer volume fraction in the adsorbed layer.

III. Comb-Copolymer Adsorption: Scaling Approach

A. Comb-Copolymer Mushroom Regime: Scaling. We now generalize our description of the adsorption of a comb polymer in a mushroom configuration ($R_t < z_1$) using a scaling approach. As in the mean field theory, the side chains give only a very small perturbation to the concentration profile and the total monomer concentration profile decays with the same power law as that of adsorbed linear polymer chains $\Phi(z) \sim z^{(1/\nu)-d}$, where $\nu \approx 0.59$ is the Flory scaling exponent and $d = 3$ is the space dimension.[23] For each of the regimes found in the mean field theory, we now derive the corresponding scaling laws.

At distances from the adsorbing surface larger than the Flory radius of the side chains $R_t \sim aN_t^{\nu}$, the side chains behave essentially as free chains. As in the mean field theory, if $R_t < z < z_1$, the density of side chains is proportional to the total monomer density and $\Phi_{sc}^{co}(z) = c_1 z^{(1/\nu)-d}$. The constant c_1 is determined by imposing the conservation of the side-chain monomers, $\int \Phi_{sc}^{co}(z)\, dz = \Gamma N_t/N_B$, leading to

$$\Phi_{sc}^{co}(z) = \frac{\Gamma N_t}{N_B R_t}\cdot\left(\frac{R_t}{z}\right)^{d-(1/\nu)}, \quad R_t < z < z_1$$

$$\rho_c^{co}(z) = \Phi_{sc}^{co}(z)/N_t \tag{27}$$

At larger distances $z_1 < z < R_B$, each loop carries one side chain, and thus $\rho_c(z) = z^{-d}$, $\Phi_{sc}^{co}(z) = N_t z^{-d}$. The crossover between these two regimes occurs at a distance z_1 given by

$$z_1 = a\left[\frac{N_B}{N_t^{\nu(d-1)-1}}\right]^{\nu} \tag{28}$$

For $d = 4$ and $\nu = 1/2$, eq 28 gives back the mean field result of section II.D, $z_1^2 = N_B/N_t^{1/2}$.

Far from the surface, for $z > R_B \sim aN_B^{\nu}$, the comb-copolymer behaves as an effective linear chain of blobs, the individual blobs being triblock copolymers with one side chain per blob and thus $\rho_c(z) = z^{-d+(1/\nu)}/N_B$, $\Phi_{sc}^{co}(z) = N_t z^{-d+(1/\nu)}/N_B$.

At short distances, $0 < z < R_t$, the density of side chain monomers is dominated by those side chains for which the junction point belongs to the same blob of size z. The density of side-chain monomers is thus equal to the product of the junction point density ρ_c by the number of monomers of the side chain in this same blob $z^{1/\nu}$, $\Phi_{sc}^{co}(z) \sim z^{1/\nu}\rho_c(z)$. To place a branching point at position z we need to place the relevant core monomer and to let a tail of size N_t start there. In contrast to the mean field description, the side-chain is correlated with the backbone. The branching point density $\rho_c^{co}(z)$ is derived in Appendix D. It is constructed from the backbone monomer density, the partition function of a free tail,[27] and the three-leg vertex at the branching point. We obtain

$$\rho_c^{co}(z) = \frac{\Gamma}{N_B R_t}\left(\frac{z}{R_t}\right)^{\alpha} \tag{29}$$

with an exponent $\alpha = -d/2 - 1 + \gamma/(2\nu) + 1/\nu - \theta_1 \simeq -0.27$. The junction points are thus weakly localized at

Table 2. Table of Symbols

Φ_b	bulk monomer volume fraction
$N = p(N_B + N_t)$	total no. of monomers per comb polymer
p	no. of triblock subunits per comb polymer
N_B	no. of backbone monomers per triblock
N_t	no. of side-chain monomers per triblock
a	monomer size (∼nm)
ϵ_o	adsorption energy per monomer of a linear chain
e	adsorption energy per monomer of a comb polymer
b	extrapolation length ($\sim 1/\epsilon_o$ for adsorbing linear chains)
$R_t = a\sqrt{N_t}$	side-chain gyration radius
$R_B = a\sqrt{N_B}$	gyration radius of backbone monomers for a triblock
z^*	thickness of loops dominated layer over the adsorbing surface
λ	total thickness of the adsorbed layer
$Z_N^o(z)$	partition function of a linear backbone adsorbing chain made of N_B monomers and with one end at position z above the adsorbing surface
$Z_N^f(z)$	partition function of a nonadsorbed linear chain of N monomers
$Z_N(z)$	partition function of a triblock made of N monomers and with one end at position z above the adsorbing surface
Γ_o	surface coverage (no. of monomers per unit surface) for a linear chain
Γ	surface coverage (no. of monomers per unit surface) for a comb polymer
L	side-chains brush vertical extension
σ	surface grafting density
d	space dimension

the surface where excluded volume correlations are screened. The des Cloizeaux exponent $\theta_1 = (\sigma_1 - \sigma_3)/\nu$ is introduced by the three leg vertex (see Appendix D). The side-chain monomer concentration can be deduced as

$$\Phi_{sc}^{co}(z) = z^{1/\nu}\rho_c(z) = \frac{\Gamma N_t}{N_B R_t}\left(\frac{z}{R_t}\right)^{\beta} \tag{30}$$

where the exponent β is close to 1.4.

Summarizing, for $R_t < z_1$, i.e. in the mushroom regime for the comb polymer, the side chains monomer volume fraction is given by

$$\Phi_{sc}^{co}(z) = \begin{cases} \dfrac{\Gamma N_t}{N_B R_t}\cdot\left(\dfrac{z}{R_t}\right)^{(-d/2)-1+(\gamma/(2\nu))+(2/\nu)-\theta_1} & 0 \le z \le R_t \\ \dfrac{\Gamma N_t}{N_B R_t}\cdot\left(\dfrac{R_t}{z}\right)^{d-(1/\nu)} & R_t \le z \le z_1 \\ \dfrac{N_t}{z^d} & z_1 \le z \le R_B \\ \dfrac{N_t}{N_B} z^{(1/\nu)-d} & R_B \le z \le \lambda_p \end{cases} \tag{31}$$

B. Comb-Copolymer Brush Regime: Scaling. So far, we have only considered the mushroom limit where the side chains do not interact. The number of side chains per unit area in the proximal layer of thickness R_t is $\sigma = \Gamma/N_B$ and the side chains interact if $\sigma {R_t}^{d-1} > 1$; in this case the side chains stretch and form a polymer brush. This occurs if $R_t \ge z_1$ or as we have shown in section II.D.1, the adsorbed combs enter the brush regime for

$$N_t \ge {N_B}^{(1/\nu(d-1))} \tag{32}$$

In the mean field approximation, ($d = 4$ and $\nu = 1/2$) this condition gives $R_t \sim {N_B}^{1/3} \sim z^*$, in agreement with our mean field results of section II.C for the crossover from the mushroom to brush configuration. We will limit our analysis to the study of strong backbone adsorption and thus we assume that the occurrence of large backbone loops with many side chains anchored is negligible.

In the brush regime, the side chains extend into the bulk from their anchoring point on the backbone in a sequence of blobs of size $D_b \sim a g^{\nu}$, where $g \sim \sigma^{-1/\nu(d-1)}$ Z_t^f is the number of monomers per blob. The grafting density is $\sigma = \Gamma/N_B$, and the blob size is $D_b \sim a {N_B}^{1/(d-1)}$. The concentration of side-chain monomers belonging to the first blob close to the surface is the same as the concentration in an adsorbed layer of comb-copolymers where the side chains would have g monomers or a radius D_b. It is obtained from the results of the previous section by replacing N_t by g and R_t by D_b. The crossover length z_1 is then given by $z_1 = a\ {N_B}^{1/(d-1)} = D_b$ and the density of side-chain monomers in the brush

$$\Phi_{sc}(z) = \frac{\Gamma}{{N_B z_1}^{1-(1/\nu)}}\cdot\left(\frac{z}{z_1}\right)^{(\gamma/2\nu)+(d-2)/2} \tag{33}$$

The thickness of the brush in the blob model is

$$L \sim a N_t\, \sigma^{(1-\nu)/(\nu(d-1))} \sim a N_t {N_B}^{-(1-\nu)/(\nu(d-1))} \tag{34}$$

The free energy of the side chains is $k_b T$ per blob or per side chain

$$F_t \sim \left(\frac{a^2}{k_b T}\right) N_t \sigma^{1/\nu(d-1)} \sim \left(\frac{a^2}{k_b T}\right) N_t {N_B}^{-1/\nu(d-1)} \tag{35}$$

The adsorption energy of the backbone chains must compensate the stretching energy of the side-chain brush. This requires an adsorption energy per monomer $\epsilon \sim F_t/N_B \sim N_t {N_B}^{-1+1/(\nu(d-1))}$. The thickness of the adsorbed backbone layer is then $\lambda_c \sim a/\epsilon^{\nu}$ or

$$\lambda_c \sim a\,\frac{{N_B}^{\nu+(1/(d-1))}}{{N_t}^{\nu}} \tag{36}$$

As the length of the side chains increases and becomes larger than $N_t \ll {N_B}^{1/(d-1)\nu}$, the thickness of the backbone adsorbed layer decreases from the radius R_B between two branching points and the adsorbed polymer amount decreases. The adsorbed layer is only stable if its thickness is larger than the proximal distance b introduced in eq 1. For longer side chains, there is no adsorption of the comb-copolymer

$$N_t \ge {N_B}^{1+(1/\nu(d-1))} \tag{37}$$

where the exponent $1 + 1/\nu(d-1)$ is equal to 11/6 for swollen chains ($d = 3$ and $\nu = 3/5$) in a good solvent.

IV. Conclusions

We propose here a theoretical investigation of the adsorption of partly adsorbing comb-copolymers, with an adsorbing skeleton and nonadsorbing side-grafts. Three regimes were identified: a "mushroom" regime characterized by having an adsorbed backbone layer on the surface and the side chains dangling from the backbone in a swollen state, a "brush" regime in which they develop a uniform multichains coating with an extended layer of nonadsorbing segments, and a nonadsorbed regime. Depending on the size of side chains, size of skeleton length between side chains, and adsorption parameters, the scaling laws for the transitions between the different regimes, the adsorption free energy and the thickness of adsorbed layers are derived using a combination of mean field and scaling approaches. In the case of swollen (ideal) chains, $\nu = 3/5$ and $d = 3$ ($\nu = 1/2$ and $d = 4$), the threshold between mushroom and brush configurations and the desorption threshold can be expressed as $N_t > {N_B}^{5/6}$ ($N_t > {N_B}^{2/3}$) and $N_t \sim {N_B}^{11/6}$ ($N_t \sim {N_B}^{5/3}$). In the brush regime we find that the thickness of the backbone adsorbed layer and the vertical extension of the brush for a swollen (ideal) chain scale as $\lambda_c \sim a {N_B}^{11/10} {N_t}^{-3/5}$ ($\lambda_c \sim a {N_B}^{5/6} {N_t}^{-1/2}$) and $L \sim a N_t {N_B}^{1-/3}$ ($L \sim a N_t {N_B}^{1-/3}$), respectively. These predictions could be checked quantitatively, by experiments able to investigate polymer adsorption, such as neutron or X-ray reflectometry, ellipsometry, quartz microbalance, or surface force apparatus, and work is currently in progress in our group in this direction. Qualitatively, this new family of copolymers can lead to rather thick layers, without the difficulty often encountered when trying to prepare long conventional (i.e. diblock or triblock) copolymers. These multiblock copolymers may thus be interesting in numerous applications, in which the adsorption of rather large objects (proteins, cells) should be prevented, or con-

trolled. They already demonstrated very interesting performances in the context of DNA sequencing and capillary electrophoresis. In this application, the interesting regime is probably the "brush" regime, because a uniform layer with no access of the analytes to the wall is wanted. The extension of the brush leads to thicker layers, which should be favorable, but also smaller adsorption free energies, so that a compromise has to be found. Most likely, a "weakly extended" brush is a good goal on the practical side. An important aspect of the problem, on the practical side, is the adsorption kinetics. It has been well recognized that the adsorption of large polymers on surfaces is strongly constrained by the kinetics of penetration of a new polymers across the already adsorbed layer, so that the thermodynamic equilibrium, which is discussed in the present article, can be hard to reach. The adsorption kinetics of high molecular weight polymers is a very difficult problem on the theoretical side, and it is beyond the scope of the present article. We believe, however, that numerous information useful for experimental development of applications can be gained from the present approach. In particular, there are practical ways to minimize kinetic barriers to adsorption, e.g., by performing adsorption from a semidilute, rather than dilute, solution.

Acknowledgment. A.S. acknowledges a "Marie Curie" Postdoctoral fellowship from the EU (HPMF-CT-2000-00940) and thanks Dr. P. Sens for very valuable discussions. This work was partly supported by a grant from Association pour la Recherche sur le Cancer (ARC).

Appendixes

A. Triblock Copolymer: Monomer Volume Fraction

$$\Phi_l(z) = \begin{cases} 2(z+d)^{-2} & 0 \le z \le z^* \\ z^{*6} z^{-8} & z^* \le z \le \lambda \end{cases}$$

$$\Phi_t(z) = \begin{cases} \frac{z}{N_B} \ln\left[\frac{z^*}{z}\right] & 0 < z < z^* \\ z^{-2} & z^* < z < \lambda \end{cases} \quad (38)$$

$$\Phi_{sc}^{TB}(z) = \begin{cases} \frac{\Gamma_o}{N_B R_t} & z^2 \quad d < z < R_t, \\ \frac{\Gamma_o R_t^3}{N_B} & z^{-2} \quad R_t < z < z^* \\ \Gamma_o R_t^3 N_B & z^{-8} \quad z^* < z < \lambda \end{cases}$$

where $z^* = (Nb \log(N/b^2))^{1/3}$.

$$\Phi^{TB}(z) = \begin{cases} 2(z+d)^{-2} + \frac{\Gamma_o}{N_B R_t} z^4 + \frac{z}{N_B} \ln\left(\frac{z^*}{z}\right) & 0 \le z \le R_t \\ \left[2 + \frac{\Gamma_o R_t^3}{N_B}\right] z^{-2} + \frac{z}{N_B} \ln\left(\frac{z^*}{z}\right) & R_t \le z \le z^* \\ z^{-2} + [z^{*6} + \Gamma_o R_t^3 N_B] z^{-8} & z^* \le z \le \lambda \end{cases} \quad (39)$$

B. Comb-Copolymer: Side Chains Monomer Volume Fraction

$$\Phi_{sc}^{co}(z) = \begin{cases} \frac{\Gamma_o}{N_B R_t} z^2 & 0 < z < R_t \\ \frac{\Gamma_o R_t^3}{N_B} z^{-2} & R_t < z < z_1 \\ \Gamma_o N_t z^{-4} & z_1 < z < R_B \\ \Gamma_o \frac{N_t}{N_B} z^{-2} & R_B < z < \lambda_p \end{cases} \quad (40)$$

C. Propagator and Partition Function of a Side Chain in a Triblock Copolymer Adsorbed Layer.

1. Chain Propagator. We calculate here the propagator of a side chain in the triblock copolymer adsorbed layer between the junction point at coordinate z_c and the free end point at coordinate z, $Z_t^f(z,N_t|z_c)$. The Laplace transform of this propagator $\tilde{Z}_t^f(z,p|\ z_c) = \int_0^\infty dN_t \exp -(pN_t)\ Z_t^f(z,N_t|z_c)$

$$-\delta(z - z_c) = \frac{\partial^2 \tilde{Z}_t^f(z,p|z_c)}{\partial z^2} - \left(p + \frac{2}{z^2}\right) \tilde{Z}_t^f(z,p|z_c) \quad (41)$$

with the boundary condition that it vanishes at the wall $z = 0$. The solution of this equation is

$$\tilde{Z}_t^f(z,p|z_c) = f_-(z_<)\, f_+(z_>) \quad (42)$$

where we have defined $z_{<,\ >} = \min, \max(z_c, z)$. The functions f_+ and f_- are given by

$$f_+(z,p) = \sqrt{\frac{\pi}{2p}}\, e^{-\sqrt{p}z} \left(1 + \frac{1}{z\sqrt{p}}\right)$$

$$f_-(z,p) = \sqrt{\frac{2}{\pi}} \left(\cosh(\sqrt{p}z) - \frac{\sinh(\sqrt{p}z)}{\sqrt{p}z}\right) \quad (43)$$

The following asymptotic limits are useful:

$$z_> \ll R_t\ \tilde{Z}_t^f(z,p=0|z_c) = \frac{z_<^2}{3z_>} \quad (44)$$

$$z_< \gg R_t\ \tilde{Z}_t^f(z,p|z_c) = \frac{1}{\sqrt{2}} e^{-\sqrt{p(z_> - z_<)}} \lim_{p\to\infty} \frac{1}{p}\, \delta(z - z_c) \quad (45)$$

2. Partition Function. The partition function of a side chain $Z_t^f(z_c)$ with the junction point at position z_c is obtained by integration of $\tilde{Z}_t^f(z,\ p|\ z_c)$:

$$\tilde{Z}_t^f(z_c,p) = f_-(z_c,p) \int_{z_c}^\infty f_+(z,p)\, dz + f_+(z_c,p) \int_0^{z_c} f_-(z,p)\, dz \quad (46)$$

At short distances from the wall $z_c \ll R_t$, the partition function is dominated by the contribution to the integral coming from $z > z_c$:

$$\tilde{Z}_t^f(z_c,p) = -\frac{z_c^2}{3} \log(\sqrt{p}z_c) \quad (47)$$

$$Z_t^f(z_c,N_t) = \frac{z_c^2}{6N_t} \quad (48)$$

At larger distances from the wall, $z_c \gg R_t$, the two integrals are equal to $^1/_2p$ and $Z(z_c, N_t) = 1$; the side chains are almost free chains.

The density of copolymer junction points $\rho_c^{TB}(z)$ and the side-chain monomers volume fraction Φ_{sc}^{TB} can be calculated using these more precise values of the propagator and partition function; one finds the following results:

$$\rho_c^{TB}(z) = \begin{bmatrix} \dfrac{1}{N_B R_t} & z \ll R_t \\ \dfrac{1}{N_B}\dfrac{R_t}{z^2} & R_t \ll z \ll z^* \end{bmatrix}$$

$$\Phi_{sc}^{TB}(z) = \begin{bmatrix} \rho_c^{TB}(z < R_t)\cdot z^2 & z \ll R_t \\ \rho_c^{TB}(z) N_t & z \gg R_t \end{bmatrix}$$

These results are similar to those obtained in the main text.

D. Density of Comb-Copolymer Branching Points. To determine using scaling arguments the density of branching points of the comb-copolymer at a distance z_c smaller than the side chain radius, we first calculate the partition function $Z_t^f(z_c, R_t)$ of a side chain with the branching point at position z_c and radius R_t.

In the limit where z_c is of the order of a monomer size a, the side chain behaves as a tail in the adsorbed layer and $Z_t^f(a, R_t) \sim R_t^{(\gamma-\nu(d-2)/2\nu)-(1/\nu)}$. We now consider the case where $z_c = R_t$. The probability to find a side chain at a distance z_c is proportional to the local monomer concentration $c(z_c) \sim z_c^{(1/\nu)-d}$. If the side chain is not connected to the backbone but is free, its partition function is $Z^o \sim z_c^{(\gamma-1)/\nu}$. The partition function of the side chain also contains a factor associated with the branching point. This is best written in terms of the vertex exponents introduced by Duplantier.[28] In the partition function of a branched polymer chain, each vertex having k legs is associated, for a chain of size z_c, to a factor $z_c^{\sigma_k/\nu}$ where σ_k is the corresponding vertex exponent. The formation of a branching point in the comb-copolymer corresponds to the disappearance of a two-legs vertex on the backbone and a one-leg vertex (the side-chain free end) and the appearance of a three-legs vertex (the branching point); it is therefore associated with a weight $z_c^{(\sigma_3-\sigma_1-\sigma_2)/\nu}$. Note that it is sufficient to consider that the backbone chain has a size z_c since, in an adsorbed polymer layer, the local screening length is the distance to the adsorbing surface z_c. Considering all these factors, we obtain the partition function

$$Z_t^f(z_c,R_t) \sim z_c^{(1-d\nu+\gamma-1+\sigma_3-\sigma_2-\sigma_1)/\nu} \sim z_c^{\gamma/\nu-d-\theta_1} \quad (49)$$

We have here used the fact that $\sigma_2 = 0$ and introduced the contact exponent $\theta_1 = (\sigma_1 - \sigma_3)/\nu \simeq 0.45$ first considered by Des Cloizeaux.[29]

The partition function $Z_t^f(z_c, R_t)$ is obtained by a scaling law extrapolating between these two asymptotic limits

$$Z_t^f(z_c,R_t) \sim z_c^{\alpha} R_t^{((\gamma-\nu(d-2))/(2\nu))-(1/\nu)} \quad (50)$$

with an exponent $\alpha = -d/2 - 1 + \gamma/2\nu + 1/\nu - \theta_1 \simeq -0.27$.

The density of branching points is proportional to this partition function; the prefactor is obtained by imposing that the total number of branching points per unit area over a thickness R_t is of order Γ/N_B:

$$\rho_c^{co}(z_c) = \frac{\Gamma}{N_B R_t}\left(\frac{z_c}{R_t}\right)^{\alpha} \quad (51)$$

References and Notes

(1) Hjerten, S.; Kubo, K. *Electrophoresis* **2000**, *14*, 390.
(2) Marshall, E.; Pennisi, E. *Science* **1998**, *280*, 994.
(3) Salas-Solano, O.; Schmalzing, D.; Koutny, L.; Buonocore, S.; Adourian, A.; Matsudaira, P.; Ehrlich, D. *Anal. Chem.* **2000**, *72*, 3129.
(4) Carrilho, E. *Electrophoresis* **2000**, *21*, 55.
(5) Viovy, J.-L. *Rev. Mod. Phys.* **2000**, *72*, 813.
(6) Ajdari, A. *Phys. Rev. Lett.* **1995**, *75*, 755.
(7) Horvath, J.; Dolnik, V. *Electrophoresis* **2001**, *22*, 644.
(8) Righetti, P. G.; Gelfi, C.; Verzola, B.; Castelletti, L. *Electrophoresis* **2001**, *22*, 603.
(9) Doherty, E. A.; Berglund, K. D.; Buchholz, B. A.; Kourkine, I. V.; Przybycien, T. M.; Tilton, R. D.; Barron, A. E. *Electrophoresis* **2002**, *23*, 2766.
(10) Liang, D.; Liu, T.; Song, L.; Chu, B. *J. Chrom.* **2001**, *909*, 271.
(11) Liang, D.; Chu, B. *Electrophoresis* **1998**, *19*, 2447.
(12) Madabhushi, R. S. *Electrophoresis* **1998**, *19*, 224.
(13) Chiari, M.; Cretich, M.; Horvath, J. *Electrophoresis* **2000**, *21*, 1521.
(14) Albarghouthi, M. N.; Buchholz, B. A.; Doherty, E. A.; Bogdan, F. M.; Zhou, H.; Barron, A. E. *Electrophoresis* **2001**, *22*, 737.
(15) Zhou, H.; Miller, A. W.; Sosic, Z.; Buchholz, B.; Barron, A. E.; Kotler, L.; Karger, B. L. *Anal. Chem.* **2000**, *72*, 1045.
(16) Barbier, V.; Buchholz, B. A.; Barron, A. E.; Viovy, J.-L. *Electrophoresis* **2002**, *23*, 1441.
(17) Joanny, J.-F.; Johner, A. *J. Phys. II* **1996**, *6*, 511.
(18) Semenov, A. N.; Bonet-Avalos, J.; Johner, A.; Joanny, J.-F. *Macromolecules* **1996**, *29*, 2179.
(19) Semenov, A. N.; Joanny, J.-F.; Johner, A. In *Theoretical and Mathematical Models in Polymer Research.* Academic Press: San Diego, CA, 1998; pp 37−82.
(20) Marques, C. M.; Joanny, J.-F. *Macromolecules* **1989**, *22*, 1454.
(21) Johner, A.; Joanny, J.-F. *Macromol. Theory Simul.* **1997**, *6*, 479.
(22) Gennes, P. G. D. *Macromolecules* **1981**, *14*, 1637.
(23) de Gennes, P. G. *Macromolecules* **1980**, *13*, 1069.
(24) Marques, C. M.; Joanny, J.-F. *Macromolecules* **1990**, *23*, 268.
(25) Marques, C. M.; Joanny, J.-F.; Leibler, L. *Macromolecules* **1988**, *21*, 1051.
(26) Grosberg, A. Y.; Khoklov, A. R. *Statistical Physics of Macromolecules*; AIP Press: New York, 1994.
(27) Semenov, A. N.; Joanny, J. F. *Europhys. Lett.* **1995**, *29*, 279.
(28) Duplantier, B. *J. Stat. Phys.* **1989**, *54*, 581.
(29) Cloizeaux, J. D.; Janink, G. *Les Polymères en Solution: leur modélisation et leur structure.* Editions de Physique: Paris, 1987.

MA0489624